



## Carbonatites and primary carbonates in the Rio Apa and Amambay regions, NE Paraguay

Piero Comin-Chiaromonti <sup>a</sup>, Angelo De Min <sup>a,\*</sup>, Vicente A.V. Girardi <sup>b</sup>, Celso B. Gomes <sup>b</sup>

<sup>a</sup> Mathematics and Geosciences Department, Trieste University, Via Weiss 8, I-34127 Trieste, Italy

<sup>b</sup> Geosciences Institute, University of São Paulo, Cidade Universitária, Rua do Lago 562, 05508-900 São Paulo, Brazil

### ARTICLE INFO

#### Article history:

Received 9 April 2013

Accepted 21 October 2013

Available online 31 October 2013

#### Keywords:

Rio Apa

Amambay regions

NE Paraguay

Carbonatite

Sub-continental mantle

### ABSTRACT

In the Rio Apa and Amambay regions, north-eastern Paraguay (NPAA), potassic, alkaline-carbonatitic rocks (138–139 Ma) predate the eruption of tholeiitic flood basalts (133 ± 1 Ma). These rocks, mainly outcropping as dykes or ring-like complexes, intrude a Cambro-Ordovician carbonate platform and Precambrian metamorphic rocks along with their Silurian and Permo-Carboniferous sediments. The main rock-types range from basanite to trachyte and trachyphonolite (and intrusive equivalents) to carbonatite, in addition to glimmeritic and pyroxenitic veins. Geological and geophysical evidence indicate that the NPAA magmatism is related to extensional tectonics, like the Early Cretaceous alkaline-carbonatitic complexes from central-eastern Paraguay (127 ± 1 Ma) and the eastern magmatic occurrences of the Paraná Basin.

Oxygen and carbon isotope compositions (whole rocks and carbonates) vary from values close to the field of continental lithospheric mantle, or that of primary carbonatites, up to values typical of a hydrothermal environment. An isotope exchange model implies that the main isotope variations, ranging from a magmatic (e.g., 1200 °C) to a low temperature (<400 °C) environment, involved fluids with CO<sub>2</sub>/H<sub>2</sub>O ratios between 0.8 and 1.0. In particular, the O–C isotopic variations, in combination with the La vs La/Yb ratios, suggest an increasingly higher level of carbonate in the silicate liquids, with increasing evolution, i.e., basanite → phonotephrite → trachyphonolite–phonolite (trachyte) → carbonatite. Sr–Nd isotopes show that the carbonatites are mantle derived without significant crustal contamination and that they can be related to isotopically enriched sources where newly formed veins (enriched component) and peridotite matrix (depleted component) underwent differing isotopic evolution.

T<sup>DM</sup> model ages for NPAA range from 1.2 to 2.3 Ga. Considering that in the whole Paraná Basin isotopically distinct K-alkaline and tholeiitic magmas were generated following the enrichment of the subcontinental mantle mainly between 1.0 and 2.3 Ga (Paleo-Mesoproterozoic events), the mantle sources preserved the isotopic heterogeneities over long time periods, suggesting a non-convective, i.e., lithospheric, mantle source beneath different cratonic or intercratonic areas.

© 2013 Elsevier B.V. All rights reserved.

## 1. Introduction

Alkaline-carbonatitic complexes are occasionally associated with predominantly tholeiitic, basaltic large igneous provinces (LIPs). Since alkaline-carbonatitic magmas represent low volume and low temperature melts, they preferentially sampled near-solidus portions of the mantle and are thus good proxies for the enriched components of LIP magmatism. Alkaline-carbonatitic complexes were emplaced both on the South American and African plates (e.g., Comin-Chiaromonti et al., 1997, 2011; Gibson et al., 2006), surrounding one of the major basaltic LIPs, the Paraná-Etendeka flood basalts of eastern South America (Brazil, Uruguay, Argentina, and Paraguay) and south-western Africa (Namibia and Angola). While most of these occurrences are coeval or postdate the main phase of tholeiitic volcanism, the magmatic

complexes reported herein are unique since they precede (by some 5 Ma) the tholeiitic magmatism of the Paraná-Etendeka flood basalts. In this study we therefore describe the main geochemical features of the ca. 138–139 Ma alkaline-carbonatitic complexes from northern Paraguay and discuss their significance for the genesis of the Paraná-Etendeka LIP and assess the relationship between the silicic and carbonatitic magmas at the eastern margin of the LIP.

### 1.1. North-eastern Paraguay magmatism

Magmatism in the Rio Apa area consists of rare occurrences of alkaline and tholeiitic dykes close to Puerto Valle-mí city (Alto Paraguay Department; Lat. 22°10'10.91"S; Long. 57°57'21.70"W), on the margins of the Paraguay River at the western part of the Precambrian "Apa High" (Livieres and Quade, 1987; cf. also Comin-Chiaromonti et al., 1999). The K-alkaline dykes (0.5–1.0 m thick; see inset Fig. 1) of basanitic to phonotephritic composition (Comin-Chiaromonti et al., 2007a,b,c

\* Corresponding author.

E-mail address: demin@units.it (A. De Min).

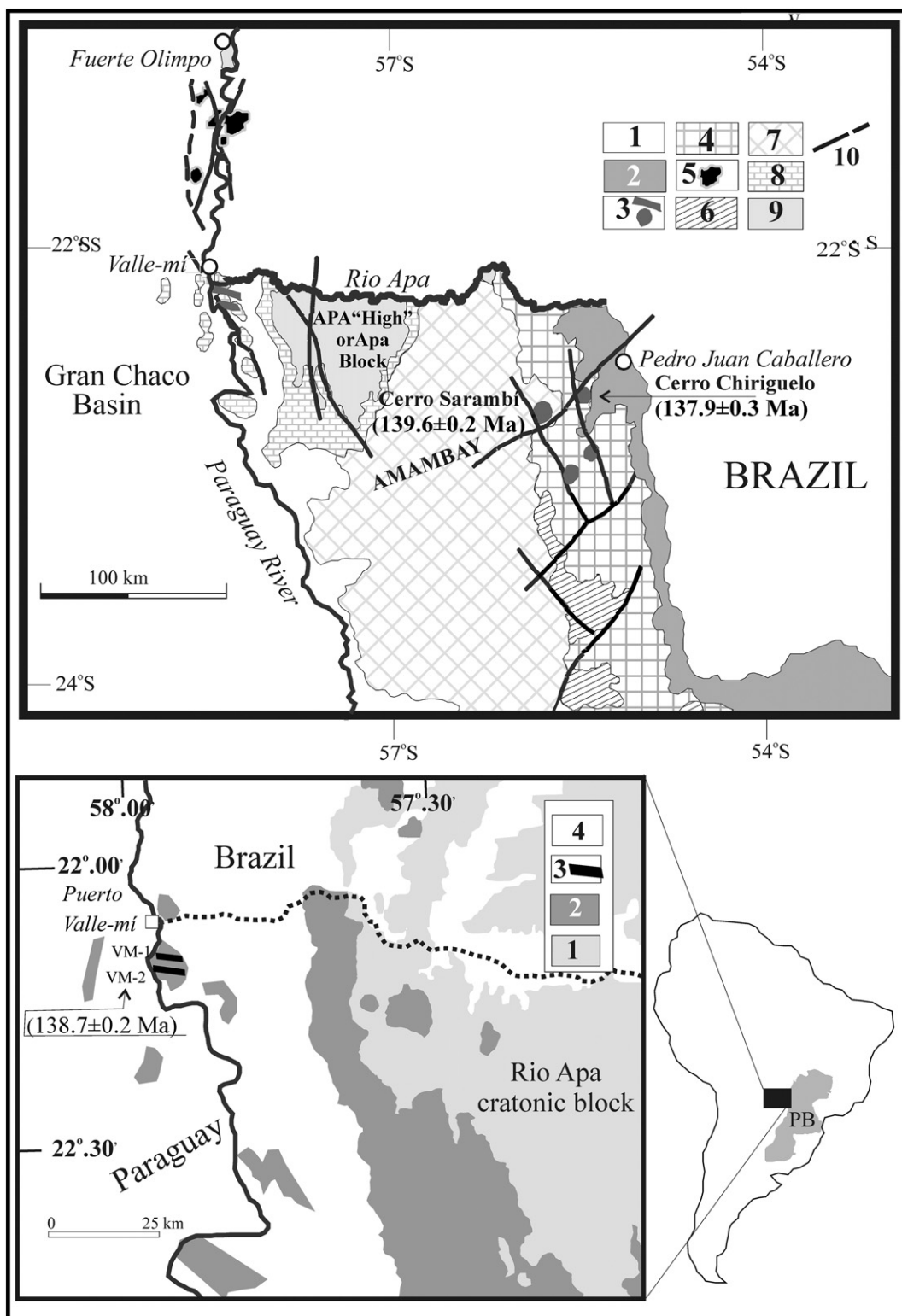


**Fig. 1.** Geological map of the northern regions of Eastern Paraguay, modified after Comin-Chiaromonti et al. (1997, 1999, 2007a)) showing the Rio Apa and Amambay Provinces. 1, Paleogene to Neogene sedimentary cover; 2, Early Cretaceous tholeites of the Paraná Basin; 3, Early Cretaceous potassic alkaline rocks (pre-tholeites, Rio Apa and Amambay Provinces); 4, Cretaceous sedimentary rocks (Misiones Formation); 5, Permo-Triassic alkaline rocks (Alto Paraguay Province); 6, Permian sedimentary rocks (Independencia Group); 7, Permo-Carboniferous sedimentary rocks (Coronel Oviedo Group); 8, Cambro-Ordovician rocks (metaterrigenous and metacarbonatic sediments of the Itacupumí Group); 9, Paleoproterozoic to Neoproterozoic crystalline basement (Apa complex, Centurion suite and San Luis Group: high- to low-grade metasedimentary rocks, metarhyolites and granitic intrusions); 10, major tectonic lineaments and faults. Inset A: sketch map of the Valle-mí region (modified after Campanha et al., 2010). 1, Proterozoic Rio Apa cratonic block; 2, Ediacaran Valle-mí metasediments; 3, Early Cretaceous basanitic dykes (VM-1, VM-2); 4, Cenozoic sedimentary cover; PB, Paraná Basin and Serra Geral Formation. The ages (Cerro Chiriguelo, Cerro Sarambí and Valle-mí) were determined by  $^{40}\text{Ar}/^{39}\text{Ar}$  dating (Comin-Chiaromonti et al., 2007a).

and references therein) intruded into a carbonate platform (ca. 480 Ma; [Cordani et al., 2005](#)), along NE-SW-trending faults. These faults were deep enough to allow the migration of primitive alkaline magmas from the mantle to the surface, across the entire block of Cambrian-Ordovician carbonate rocks at 138–139 Ma. This magmatic event predates the emplacement of tholeiitic dykes at 133 Ma ([Comin-Chiaromonti and Gomes, 2005](#) and references therein, as well as [Comin-Chiaromonti et al., 2007a,b,c](#)) in the region (Paraná Basin, Serra Geral Formation; PB of [Fig. 1](#)), which comprise both high- and low-Ti variants.

In the Amambay region ([Figs. 1, 2](#)), the alkaline magmatic activity is mainly represented by the ring-like complexes of Cerro Chiriguelo and Cerro Sarambí (both with occurrences of carbonatite facies; cf., [Fig. 2](#) and [Comin-Chiaromonti et al., 1999](#)), lying on the border between Brazil and Paraguay, along the Jejui-Aguaray-Guazu fault system, an important N35°E trending structural belt ([Livieres and Quade, 1987](#)).

Trachytic and phonolitic dykes occur in the region, and pyroxenite and glimmerite veins (with cumulate textures) are present in the Cerro Sarambí area ([Castorina et al., 1997](#)). Ar–Ar dating yielded an age of  $139 \pm 2$  Ma, which is similar to the K/Ar age of the Rio Apa basanitic dykes ( $138 \pm 7$  Ma; [Castorina et al., 1997](#)). Additional field evidence, i.e., overlapping tholeiitic flows, support an age older than 133 Ma for the alkaline occurrences ([Fig. 2](#)), which are however similar in composition to the post-tholeiitic potassiac magmatism from the Asunción-Sapucay-Villarrica graben, central Paraguay (126–129 Ma; [Comin-Chiaromonti et al., 2007a](#)).

Thus, the Rio Apa and Amambay regions are characterized by near-coeval magmatism, with the least differentiated rocks occurring in the Rio Apa (mg# 0.64–0.66), and are carbonate rich (see [Comin-Chiaromonti et al., 2005a](#)). In particular, parental CO<sub>2</sub>-rich basanitic magmas may have fractionated under virtually closed system conditions, with an evolutionary trend from basanite to phonotephrite,

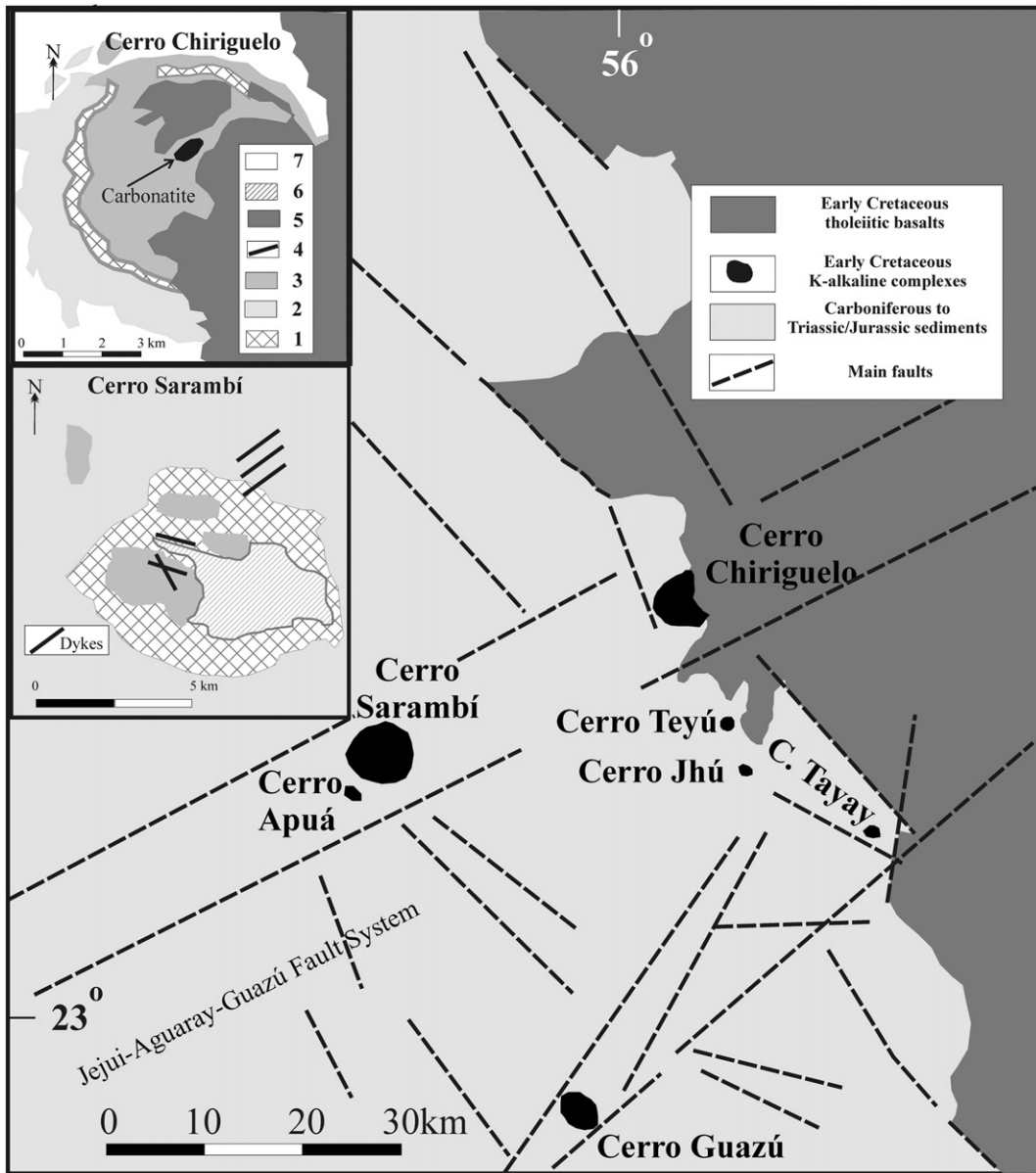


**Fig. 2.** Detailed sketch of the Amambay region (after [Comin-Chiaromonti et al., 1999](#); [Gomes et al., 2011](#)). Insets: Cerro Chiriguelo and Cerro Sarambí complexes (after [Comin-Chiaromonti et al., 2005a, 2005b](#)). 1, Precambrian crystalline basement; 2, Cambrian to Jurassic sediments, granitic intrusions and quartz-porphyritic lavas; 3, Early Cretaceous K-alkaline rock-types (Pre-tholeiites); 4, Early Cretaceous tephritic to phonolitic-carbonatitic dykes; 5, Early Cretaceous flood tholeiites; 6, Cretaceous conglomerates; 7, Tertiary-Quaternary alluvial cover.

trachyphonolite, trachyte/phonolite and finally carbonatite (Comin-Chiaromonti et al., 2005b).

## 2. Classification and nomenclature

The nomenclature for silicate rocks from north-eastern Paraguay, Apa and Amambay regions (NPAA) is based on their bulk geochemical composition, using the TAS (after Le Maitre, 1989; cf. Fig. 3) and De La Roche classification schemes (De la Roche et al., 1980) (cf. Tables 1 to 3). Rock-types include basanites, tephrites, phonotephrites, tephriphonolites, trachytes and trachyphonolites (glimmerites are not plotted), and have a potassic affinity (according to the inset of Fig. 3). The carbonatites are mainly sōvites and alvikites. For comparison, the compositions of post-alkaline tholeiites and of the crystalline basement are also plotted.

## 3. Petrographic observations

Selected samples include the main rock-types of the Rio Apa (Valle-mí), Cerro Chiriguelo and Cerro Sarambí areas (cf. Comin-Chiaromonti et al., 1996, 2005; Piccirillo and Melfi, 1988 and references therein).

### 3.1. Rio Apa–Valle-mí

Basanitic dykes are only found in the Rio Apa region intruding a carbonate platform and are characterized by chilled margins, less than 1.0 mm thick, consisting of microcrystalline carbonates. The basanites are fine- to medium-grained, porphyritic, mesocratic rocks with up to 30 vol.% phenocrysts and microphenocrysts of euhedral to subhedral olivine ( $Fo_{84-86}$ ), clinopyroxene ( $Wo_{45-48}En_{42-47}Fs_{8-12}$ ), and tetraferriphlogopite ( $mg\#$  up to 0.74;  $mg\# = Mg/Mg + Fe$ ). The microcrystalline groundmass consists of clinopyroxene, primary carbonates (up to 20 vol.%), alkali feldspar, foids and magnetite. Accessory minerals are apatite, titanite and perovskite; the latter are found near or in the carbonatic fraction.

Tephritic dykes are porphyritic with phenocrysts and microphenocrysts of olivine ( $Fo_{72-79}$ ), clinopyroxene ( $Wo_{44-49}En_{40-48}Fs_{9-14}$ ), rare zoned plagioclase ( $An_{20-70}$ ) and pseudoleucite. The groundmass is microcrystalline, consisting of microlites of olivine ( $Fo_{70-72}$ ), clinopyroxene ( $Wo_{47-48}En_{38-40}Fs_{12-15}$ ), calcite (up to 10 vol.%), plagioclase ( $An_{14-20}$ ), alkali feldspar ( $Or_{65-70}$ ), Ti-magnetite, analcime, biotite ( $mg\#$  0.65), pargasite, apatite and titanite.

Tholeiitic dykes also intrude the carbonate platform and show chilled margins strongly enriched in epidote (clinozoisite up to  $mg\#$  0.64 and  $Fe^{3+}/(Fe^{2+} + Al) = 0.03$ ). The ST-1 dyke (tholeiitic basalt; cf. Tables 1–3) has a subophitic, holocrystalline texture with olivine ( $Fo_{61}$ ), clinopyroxene ( $Wo_{33-35}En_{38-49}Fs_{16-29}$  to  $Wo_{8-10}En_{55-59}Fs_{30-33}$ ), plagioclase ( $An_{52-64}$ ), titanomagnetite (ulvöspinel ~72%), and interstitial quartz, as well as accessory biotite and apatite. The ST-2 dyke (basaltic andesite) has a porphyritic texture with phenocrysts of plagioclase ( $An_{50-68}$ ), clinopyroxene, opaques and olivine. The groundmass is seriate and made of plagioclase ( $An_{40-51}$ ), clinopyroxene ( $Wo_{34}En_{38}Fs_{28}$  and  $Wo_{8}En_{55}Fs_{37}$ ), quartz-alkali feldspar micrographic intergrowths, opaques (titanomagnetite: ulvöspinel up to 94%), olivine ( $Fo_{42-43}$ ) and apatite.

Carbonate rocks from the carbonate platform, such as samples PS-279 and PS-280 are microsparitic dolomite and well recrystallized sparitic calcite (with ghosts of fossil remains), respectively. A Cambro-Ordovician age (500–480 Ma) was determined by Palmieri and Velázquez (1982) for these rocks.

### 3.2. Cerro Chiriguelo complex

Trachytic rocks surround a central sōvitic core and appear to be fenitized (cf. Censi et al., 1989). Massive fenites have a porphyritic texture with phenocrysts of sanidine ( $Or_{94-97}$ ) and microphenocrysts of sanidine, aegirinic clinopyroxene ( $Ae_{45}Wo_{24}En_{12}Fs_{19}$ ), biotite ( $mg\#$  0.70), occasional garnet (andradite up to 81 mol%) and magnetite set in a groundmass, consisting of the same phases, plus glass and secondary patches of goethite–limonite. Apatite is a common accessory mineral. Uranpyrochlore, strontian loparite and strontio-chevkinite are occasionally present (Haggerty and Mariano, 1983). Fenitic dykes also have a trachytic texture and show a weak porphyritic texture with phenocrysts and microphenocrysts of sanidine set in a groundmass made of glass, sanidine, aegirine, opaques and accessory apatite.

Carbonatites in the core of the complex (Fig. 2) are sōvite (C1 stage, according to the nomenclature of Le Bas, 1981) and have, on the whole, a medium- to coarse-grained subhedral–granular texture. However, veins through the sōvites have fine-grained aplitic textures (C2 stage). Quartz, phlogopite, barite, sanidine, apatite, dolomite, uranpyrochlore, magnetite, aegirine, zircon, strontianite, synchysite, haematite, goethite and pyrite may be present. Quartz, barite and uranpyrochlore are related to late phases, filling fractures. Finally, fenitic dykes and ferrocarbonatite veins (C3 stage) cross-cut carbonatites C1 and C2 (Censi et al., 1989).

Tholeiitic basaltic andesites (Bellieni et al., 1986), covering the eastern limb of the complex have textural and mineralogical characteristics similar to those described for the Valle-mí ST-2 dyke.

Finally, rare banded rocks (gneisses), occurring as xenoliths in the trachytes and composed mainly of quartz, microcline and plagioclase with subordinate biotite and muscovite (e.g., sample CC-G of Table 2), are believed representative samples of the Precambrian crystalline basement (see Cordani et al., 2005, 2010).

### 3.3. Cerro Sarambí complex

The main rock-types are syenites-syenodiorites crosscut by phonotepitic, sōvitic and silico-sōvitic dykes, as well by glimmeritic and pyroxeenitic veins. Trachytic-trachyphonolitic satellite plugs are present (Castorina et al., 1997; Comin-Chiaromonti and Gomes, 1996), the largest one being Cerro Apuá (Gomes et al., 2011).

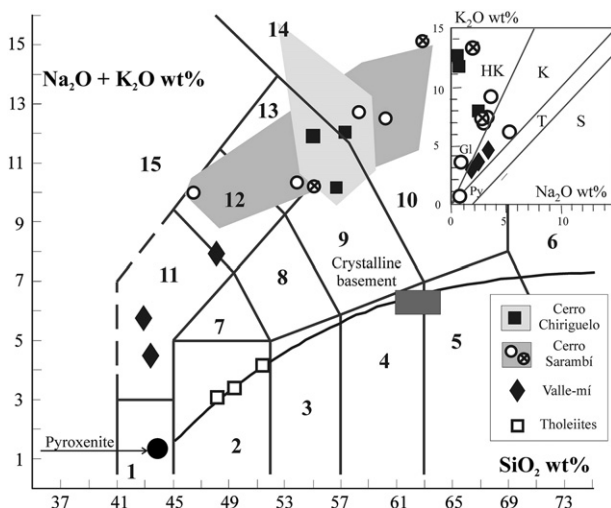


**Fig. 3.** Total alkalis vs. silica plot for representative alkaline rocks, tholeiitic basalts and gneissic basement from the Rio Apa and Amambay regions. The grey fields represent the composition of the whole alkaline population of Cerro Chiriguelo and Cerro Sarambí, as taken from Censi et al. (1989), Castorina et al. (1997) and Gomes et al. (2011). Classification fields are as follows: 1, picrobasalt; 2, basalt; 3, basaltic andesite; 4, andesite; 5, dacite; 6, rhyolite; 7, trachybasalt; 8, basaltic trachyandesite; 9, trachyandesite; 10, trachyte; 11, tephrite (olivine <10 wt%); 12, basanite (olivine >10 wt%); 13, tephriphonolite; 14, phonolite; 15, foidite. Inset:  $Na_2O$  vs  $K_2O$ : HK, highly potassic; K, potassic; T, transitional; S, sodic.

**Table 1**

Representative samples of rock-types from the Rio Apa region: Valle-mí L-Ti and H-Ti = low (<2.0 wt.%) and high (>2.0 wt.%) TiO<sub>2</sub> content; WR = whole rock; CF = carbonate fraction; IR = insoluble residuum; R1 = 4Si-11(Na + K)-2(Fe + Ti); R2 = 6Ca + 2 Mg + Al; "m" and "i", measured and initial (138 Ma) isotopic ratios.

VALLE-MI Rock-type	Basanite	Basanite	Basanite	Tephrite	Tephrite	Thol. basalt L-Ti	Thol. Andesi basalt H-Ti	Carbonatic Platform Dolostone	Carbonatic Platform Limestone
Sample	VM-1	VM-1	VM-2	VM-3	VM-3	ST-1	ST-2	PS279	PS280
	IR	CF(15%)	WR	IR	CF(11%)	WR	WR	WR	WR
<i>wt.%</i>									
SiO <sub>2</sub>	42.90		43.38	47.96		48.23	51.49	0.01	
TiO <sub>2</sub>	3.59		2.87	2.44		1.44	2.42	–	
Al <sub>2</sub> O <sub>3</sub>	12.13		10.20	15.14		16.20	15.36	0.04	
Fe <sub>2</sub> O <sub>3</sub>	2.12		1.50	4.04		1.95	2.02	–	
FeO	10.39	0.29*	11.30	7.90	0.80*	10.57	10.40	0.02*	
MnO	0.22		0.20	0.17		0.17	0.20	–	
MgO	10.10	0.20	12.08	6.15	0.62	7.51	4.13	20.69	55.80
CaO	11.72	6.67	11.17	8.26	5.26	8.59	6.80	31.31	
Na <sub>2</sub> O	2.32		1.58	3.29		2.52	3.04	–	
K <sub>2</sub> O	3.53		2.91	4.65		0.74	1.24	–	
P <sub>2</sub> O <sub>5</sub>	0.68		0.54	0.49		0.20	0.37	–	
CO <sub>2</sub>	–	8.13	–	4.13	–	–	47.16	43.78	
LOI	–	–	2.22	–	–	1.58	2.48	–	
Sum	99.70	15.39	99.98	100.00	10.81	99.70	99.95	99.23	99.58
mg#	0.64		0.66	0.58		0.56	0.41		
Age (Ma)	139		139	139		133	133	480	480
R1	775		1281	568		1764	1658	–	–
R2	1993		2101	1539		1609	1234	–	–
<i>ppm</i>									
Cr	253		317	154		251	28	–	–
Ni	89		101	59		119	17	–	–
Rb	40.6	0.90	41.8	62	2.6	29.1	39	4.9	7.3
Ba	1245	435	973	1743	285	301	463	9.4	14.4
Th	19.5		19.0	23.6		2.16	6.5	0.12	0.04
U	5.0		4.2	6.1		0.95	1.5	0.03	0.34
Ta	4.6		4.5	5.6		0.55	1.1	0.04	0.03
Nb	61.5		47.6	74.3		4.02	16	0.73	0.10
Sr	1151	12846	1171	1804	2511	376	395	272	2670
Hf	9.3		4.7	11.9		2.80	6.9	0.31	0.13
Zr	364		203	465		109	240	–	–
Y	27.3		23.0	36.2		31	52	0.90	1.3
La	149	155	156.6	120	125	12	23.1	1.05	0.86
Ce	315	340	309.2	254	271	39	53.1	1.54	1.08
Pr	38.9	43.5	40.0	31.4	34.7	4.9	6.5	0.15	0.13
Nd	148.7	168.2	147.3	119.0	130	14.0	28.3	1.42	0.47
Sm	23.8	27.7	24.3	19.1	20.8	3.54	6.8	0.32	0.10
Eu	5.89	10.65	6.30	4.72	7.83	1.21	2.52	0.03	0.13
Gd	17.85	33.12	20.71	14.38	24.9	3.95	8.26	0.11	0.24
Tb	1.47	5.24	3.20	1.19	3.89	0.67	1.36	0.02	0.03
Dy	8.34	30.0	17.60	6.86	21.8	3.91	7.95	0.09	0.11
Ho	1.49	5.45	3.12	1.29	3.76	0.72	1.44	0.020-	0.024-
Er	3.78	12.27	9.23	3.28	8.65	2.16	4.31	0.04	0.08
Tm	0.49	1.34	0.96	0.42	0.98	0.27	0.66	0.01	0.005
Yb	2.61	5.95	5.20	3.66	3.98	2.11	4.48	0.03	0.06
Lu	0.30	0.67	0.61	0.42	0.45	0.39	0.63	0.008-	0.004
La/Yb	57.1	26.1	30.1	32.8	31.4	5.7	5.2	35.0	14.3
$\delta^{18}\text{O}$		8.53			8.02			20.55	22.85
$\delta^{13}\text{C}$		–6.82			–7.50			–0.27	0.57
$^{87}\text{Rb}/^{86}\text{Sr}$	0.102418	0.00020	0.10326	0.09943	0.00299	0.22388	0.28561	0.05213	0.00791
$(^{87}\text{Sr}/^{86}\text{Sr})\text{m}$	0.707165(6)	0.706904(1)	0.707162(6)	0.707155(9)	0.706480(1)	0.706285(6)	0.706249(6)	0.70873(2)	0.70858(2)
$^{147}\text{Sm}/^{144}\text{Nd}$	0.09675	0.11123	0.13009	0.09702	0.09672	0.15285	0.14525	0.13622	0.1286
$(^{143}\text{Nd}/^{144}\text{Nd})\text{m}$	0.511937(9)	0.511950(9)	0.511967(8)	0.511938(9)	0.511887(11)	0.512513(8)	0.512467(7)	0.512168(9)	0.51208(1)
$(^{87}\text{Sr}/^{86}\text{Sr})\text{i}$	0.706965	0.706904	0.706954	0.706960	0.706474	0.705862	0.705709	0.70837	0.70852
$(^{147}\text{Nd}/^{147}\text{Nd})\text{i}$	0.511800	0.511860	0.511876	0.511850	0.511799	0.512380	0.512341	0.51174	0.51168
$\epsilon^{\text{Sr}}$	37.26	36.40	37.19	37.20	30.31	21.52	19.36	60.10	62.26
$\epsilon^{\text{Nd}}$	–11.92	–11.71	–11.37	–11.90	–12.88	–1.69	–2.46	–5.47	–6.72
T <sup>DM</sup>	1513	1534	1513	1516	1584	1435	1415	1809	1805

Syenites-syenodiorites are allotriomorphic to porphyritic with alkali feldspar (~Or<sub>73</sub>Ab<sub>27</sub>) and clinopyroxene phenocrysts (Wo<sub>48–49</sub>En<sub>36–40</sub> Fs<sub>11–14</sub>) set in a medium-grained groundmass consisting of alkali feldspar (Or up to 82 mol%), clinopyroxene (augite with aegirinic component up to 20 mol%), nepheline (kalsilite component around

20 mol%), mica (phlogopite–annite series with mg# 0.68), occasional garnet (andradite up to 86 mol%) and accessory apatite, titanite, opaques and zircon.

Phonotephritic dykes are porphyritic in texture, similar to the tephritic dykes from Rio Apa, with pheno- and microphenocrysts of

**Table 2**

Representative samples of rock-types from Amambay area, Cerro Chiriguelo complex. Abbreviations as in Table 1.

Amambay Chiriguelo Rock-type	Trachyte	Trachyte	Trachyte	Carbonatite	Carbonatite	Thol, Andesi basalt	Crystalline basement Gneisses
Sample	3423	3424	24-71	3422	3434	B989	CC-G
	WE	WR	WR	CF	WR	WR	WR
<i>wt.%</i>							
SiO <sub>2</sub>	55.24	56.98	56.93	5.05	7.18	49.16	61.74
TiO <sub>2</sub>	1.34	1.11	0.80	0.010	0.10	2.13	0.82
Al <sub>2</sub> O <sub>3</sub>	17.63	16.96	16.85	0.30	0.56	14.11	16.06
Fe <sub>2</sub> O <sub>3</sub>	2.86	2.02	2.75	3.54**	0.32	4.70	1.08
FeO	6.29	6.17	4.93	–	2.70	8.77	5.66
MnO	0.37	0.25	0.08	0.28	0.15	0.20	0.11
MgO	2.02	1.65	1.70	0.41	0.50	5.24	2.57
CaO	1.92	1.59	2.38	47.00	46.98	9.18	3.25
Na <sub>2</sub> O	0.26	0.20	2.36	0.03	0.04	2.39	2.75
K <sub>2</sub> O	11.61	12.53	7.74	0.28	0.50	0.97	3.78
P <sub>2</sub> O <sub>5</sub>	0.06	0.08	0.18	0.69	0.48	0.28	0.31
CO <sub>2</sub>	–	–	–	38.29	38.05	–	–
LOI	2.27	1.23	3.14	–	–	1.89	1.43
Sum	99.60	100.77	99.84	95.97	97.86	99.02	99.56
mg#	0.36	0.32	0.38	–	–	0.52	0.45
Age (Ma)	138	138	138	138	138	130	1750?
R1	530	545	918	–	–	1782	2045
R2	651	585	670	–	–	1519	790
<i>ppm</i>							
Cr	45	20	33	10	6	119	29
Ni	12	11	8	16	9	103	11
Rb	218	256	328	39	36	18	114
Ba	4478	3069	5334	22123	10390	214	601
Th	38	25	30.9	22	28	2.27	10.9
U	5.0	5.0	4.1	10	9.6	0.53	1.7
Ta	5.4	4.8	7.5	8.04	7.6	0.76	1.0
Nb	138	124	185	178	100	11	17.1
Sr	500	543	863	5243	7441	273	375
Hf	19.0	12.9	13.2	5.1	10	4.8	4.9
Zr	870	598	601	219	430	167	163
Y	56	44	39	9.8	10	10.8	24
La	813	633	721	1169	590	23	38.5
Ce	733	489	598	1102	633	52	75.1
Pr	96	64.1	80	101	63.1	6.3	8.9
Nd	405	358	365	178	120	19.3	28.55
Sm	77.0	64.1	70.6	30	20.1	4.1	6.61
Eu	16.5	13.7	14.6	10.2	6.9	1.48	1.40
Gd	79.2	65.8	72.3	32.4	21.8	4.9	8.01
Tb	12.4	8.5	10.1	5.2	3.6	0.82	0.6
Dy	69.8	47.3	58.3	31.0	21.2	4.8	5.32
Ho	12.1	8.3	9.9	5.87	4.06	0.88	1.41
Er	26.9	11.4	18.9	14.2	9.9	2.64	3.36
Tm	2.71	1.13	2.1	1.71	1.23	0.37	0.40
Yb	8.15	7.07	7.75	8.04	6.03	2.71	1.78
Lu	1.16	0.98	1.01	0.77	0.68	0.44	0.27
La/Yb	99.7	90.4	93.0	145.4	97.8	8.5	16.3
δ <sup>18</sup> O	18.04			12.48	11.22		
δ <sup>13</sup> C	–6.89			–7.26	–6.52		
<sup>87</sup> Rb/ <sup>86</sup> Sr	1.26168	1.36431	1.09984	0.00872	0.01400	0.19073	0.88148
( <sup>87</sup> Sr/ <sup>86</sup> Sr)m	0.709660(2)	0.709864(2)	0.709342(10)	0.707215(10)	0.707220(10)	0.70601(2)	0.73020(2)
<sup>147</sup> Sm/ <sup>144</sup> Nd	0.11493	0.10823	0.11692	0.12490	0.10075	0.12841	0.13995
( <sup>143</sup> Sm/ <sup>144</sup> Nd)m	0.511718(3)	0.511713(5)	0.511716(7)	0.511728(7)	0.511706(9)	0.512421	0.511648
( <sup>87</sup> Sr/ <sup>86</sup> Sr)i	0.707185	0.707188	0.707184	0.707198	0.707190	0.70566	0.70802
( <sup>143</sup> Sm/ <sup>144</sup> Nd)i	0.511614	0.511615	0.511610	0.511615	0.511610	0.512311	0.51004
ε <sup>7</sup> Sr	40.40	40.43	40.39	40.58	40.47	18.58	76.48
ε <sup>7</sup> Nd	–16.51	–16.49	–16.59	–16.49	–16.50	–3.10	–6.60
T <sup>DM</sup>	2095	1976	2139	2300	1860	1230	2238

clinopyroxene, biotite, plagioclase set in a hypocrystalline groundmass with alkali feldspar, clinopyroxene, biotite, foids and accessory apatite, zircon and titanite.

Trachytes and trachyphonolites display aphyric to porphyritic textures with alkali feldspar (Or<sub>85–88</sub>), feldspathoids (mainly nepheline), clinopyroxene (Wo<sub>48–49</sub>En<sub>26–39</sub>Fs<sub>13–25</sub>) and biotite (mg# 0.60–0.65) as

pheno- to microphenocrysts, set in a hypohyaline groundmass formed by the same minerals plus glass. In the trachyphonolitic rocks primary calcite may be an important phase (up to 7–10 vol.%).

Glimmeritic veins are inequigranular rocks with prevailing phlogopite/tetraferriphlogopite (up to 60 vol.% with mg# 0.70–0.80), subordinate calcite (up to 25 vol.%) and diopsidic clinopyroxene (about 5%,

**Table 3**

Representative samples of rock-types from Amambay area, Cerro Sarambí complex. Abbreviations as in Table 1.

AMAMBAY SARAMBÍ Rock-type	Glimmeritic Carb. dyke*	Carbonate fraction: (dolomite) 27%	Pyroxenite vein	Phono tephrite dyke	Syenodiorite	Syenite	Trachyte plug	Trachy phonolite Cerro Jhú	Carbonate fraction (calcite) 7%	Trachy Phonolite Cerro Teyú
Sample	GL-SA	GL-SA	Z1-A	P56(°°°)	PS49(°°°)	P46(°°°)	P34(°°°)	SA-95B	SA-95B	P17(°°°)
	WR	DOL	WR	WR	WR	WR	WR	WR	CALC	WR
wt%										
SiO <sub>2</sub>	28.82	—	43.50	46.41	54.99	63.03	59.94	53.73	—	57.98
TiO <sub>2</sub>	3.32	—	2.08	1.65	1.86	0.25	0.61	0.81	—	0.42
Al <sub>2</sub> O <sub>3</sub>	7.37	—	5.06	14.55	11.76	17.71	16.63	14.04	—	16.93
Fe <sub>2</sub> O <sub>3</sub>	2.11	—	2.10	9.04**	8.73**	1.56**	3.89**	1.58	—	4.43**
FeO	6.81	1.49*	8.10	—	—	—	—	5.26	4.25	—
MnO	0.11	—	0.20	0.16	0.15	0.03	0.08	0.11	—	0.22
MgO	19.27	20.89	17.85	3.03	3.06	0.27	0.62	1.46	3.95	1.37
CaO	9.23	30.21	17.75	7.35	6.24	1.00	2.66	5.99	48.17	5.72
Na <sub>2</sub> O	0.29	—	0.63	2.96	2.74	1.77	5.25	3.02	—	3.44
K <sub>2</sub> O	3.35	—	0.79	7.07	7.39	13.33	6.25	7.35.	—	9.36
P <sub>2</sub> O <sub>5</sub>	0.31	—	0.12	0.66	0.76	0.12	0.18	0.32	—	0.07
CO <sub>2</sub>	12.82	47.41	0.57	—	—	—	—	2.98	43.63	—
H <sub>2</sub> O*	3.39	—	0.60	—	—	—	—	0.79	—	—
F	1.23	—	—	—	—	—	—	0.45	—	—
LOI	—	—	7.07	1.10	0.88	2.81	—	—	—	2.72
Sum	99.43	100.00	99.35	99.94	98.78	99.64	98.81	97.89	100.00	99.40
mg#	0.83	—	0.80	0.44**	0.44**	0.29**	0.27**	0.33	—	0.12**
Age (Ma)	139	139	139	139	139	139	139	139	139	139
R1	—	—	2157	120	697	409	556	582	—	—226
R2	—	—	2884	1222	1050	468	642	989	—	565
ppm										
Cr	321	—	2045	—	54	23	35	44	—	15
Ni	185	—	676	—	14	15	6	18	—	—
Rb	138.1	6.7	9.9	91.27	146	188	110	145	16.9	165.1
Ba	2082	—	405	3688	4856	3482	2845	3624	—	4536
Th	12.5	—	1.7	23.3	19.8	8.3	29.5	37.6	—	47.6
U	3.9	—	0.5	5.1	3.9	2.1	6.6	7.8	—	11.4
Ta	7.7	—	1.6	4.0	4.0	0.8	3.6	2.9	—	1.8
Nb	94	—	18.3	76	59	33	79	95	—	93
Sr	1387	2860	870	6249	2258	1979	2028	2677	4066	2083
Hf	7.1	—	4.9	13.7	9.9	3.9	13.0	17.4	—	18.7
Zr	289	—	111	514	423	147	454	607	—	824
Y	23	—	21	22	32	6	19	36	—	22
La	167	513	65	205	194	57.8	154	239	343	146
Ce	319	980	89	379	379	101	267	456	654	237
Pr	35.6	45.3	8.8	40.5	42.4	9.81	28.6	36.6	41	21.6
Nd	123.0	139	21.0	144	154	33.3	88.3	137	138	62.7
Sm	14.7	20.1	2.8	18.3	20.6	4.16	10.84	16.4	18.3	8.1
Eu	3.9	6.1	0.81	4.97	5.13	1.02	2.94	4.4	5.25	1.90
Gd	10.1	19.3	2.0	10.4	12.5	2.3	6.4	15.3	10.4	4.8
Tb	1.03	2.14	0.21	1.1	1.5	0.3	0.8	1.3	1.65	0.7
Dy	7.6	12.9	1.61	5.2	7.1	1.3	3.8	10.8	8.7	3.6
Ho	1.1	2.51	0.19	0.8	1.1	0.2	0.6	1.4	1.9	0.7
Er	2.9	6.27	0.85	2.1	3.1	0.6	2.0	3.8	4.8	2.4
Tm	0.4	0.68	0.08	0.27	0.39	0.08	0.26	0.52	0.53	0.38
Yb	1.7	3.28	0.73	1.7	2.5	0.5	1.8	2.9	2.53	2.5
Lu	0.23	0.43	0.05	0.21	0.32	0.06	0.24	0.40	0.34	0.36
La/Yb	98.2	156.4	89.0	120.0	77.6	115.6	85.6	82.4	135.6	58.4
δ <sup>18</sup> O	—	7.04	—	—	—	—	—	—	14.89	—
δ <sup>13</sup> C	—	-8.61	—	—	—	—	—	—	-6.40	—
( <sup>87</sup> Rb/ <sup>86</sup> Sr)m	0.28808	0.00678	0.03292	0.04213	0.18709	0.27485	0.15693	0.15671	0.01202	0.22607
( <sup>87</sup> Sr/ <sup>86</sup> Sr)m	0.70803(1)	0.70747(1)	0.707525(6)	0.70721(1)	0.70831(1)	0.70785(1)	0.70779(1)	0.707769(7)	0.707483(6)	0.70792(1)
( <sup>143</sup> Sm/ <sup>144</sup> Nd)m	0.07224	0.08741	0.08060	0.07661	0.08086	0.07551	0.07421	0.07236	0.08016	0.07809
( <sup>143</sup> Sm/ <sup>144</sup> Nd)m	0.511632(3)	0.511648(4)	0.511639(7)	0.511653(9)	0.511676(9)	0.511643(9)	0.511659(8)	0.511632(7)	0.511629(8)	0.511714(7)
( <sup>87</sup> Sr/ <sup>86</sup> Sr)i	0.70746	0.70745	0.70746	0.70713	0.70794	0.70731	0.70748	0.70754	0.70746	0.70747
( <sup>143</sup> Sm/ <sup>144</sup> Nd)i	0.51157	0.51157	0.51156	0.51158	0.511602	0.511574	0.51159	0.51156	0.51156	0.51164
ε <sup>T</sup> Sr	44.33	44.26	44.32	39.58	51.12	42.14	44.60	45.45	44.30	44.50
ε <sup>T</sup> Nd	-17.42	-17.39	-17.43	-17.09	-16.66	-17.27	-16.93	-17.42	-17.64	-15.93
T <sup>DM</sup>	1577	1739	1663	1602	1623	1601	1570	1578	1669	1554

mg# ~0.80). Accessory minerals are magnetite, apatite, fluorocarbonates, titanite, and perovskite. Notably, the glimmerites are characterized by presence of ocelli (Fig. 7).

Pyroxenitic veins are essentially medium-grained cumulates of diopside (mg# 0.75–0.80) with interstitial phlogopite, alkali feldspar, magnetite, carbonates, titanite and apatite.

Finally, it should be noted that Castorina et al. (1996, 1997) also described in the complex *søvitic* and silico-*søvitic* veins and stringers bearing fluorite, fluorocarbonates, vermiculite and opaques as accessories.

#### 4. Materials and methods

Geochemical analyses of the K-alkaline rocks from the Valle-mí region, and from the Cerros Chiriguelo and Sarambí complexes are listed in Tables 1, 2 and 3, respectively. For comparison, analyses of tholeiitic dykes and flows (post K-alkaline magmatism), carbonate platform and crystalline basement rocks are also reported. Major and some trace elements (Cr, Ni, Ba, Rb, Sr, Zr, Y) were analyzed at the University of Trieste by X-ray fluorescence (Philips PX 1400) using fused and pressed powder discs. H<sub>2</sub>O was determined by Karl-Fischer-titration and CO<sub>2</sub> was measured by colorimetric methods (following Rowell, 1995). FeO was

determined by titration, and F by ion-selective electrode; total iron as Fe<sub>2</sub>O<sub>3</sub>. Trace elements (including rare earth elements) were determined by ICP-MS (inductively coupled plasma mass spectrometry) at the Acmelab, Canada (some analyses, indicated by an asterisk in the data Tables 1–3 are from Gomes et al., 2011).

Carbonates for carbon and oxygen isotope analyses were reacted in duplicate with 100% H<sub>3</sub>PO<sub>4</sub> at 25 °C for one day and three days (calcite and dolomite, respectively) and analyzed by means of a Finnigan Mat Delta E mass spectrometer at the University of Trieste. The results are given in terms of the conventional δ‰ units; the reference standards were PDB-1 and V-SMOW for C and O isotopic compositions, respectively. The <sup>87</sup>Sr/<sup>86</sup>Sr and <sup>143</sup>Nd/<sup>144</sup>Nd isotopic analyses were performed at Pisa (Istituto di Geocronologia e Geologia Isotopica; CNR) and at Napoli (Istituto di Geofisica e Vulcanologia, Università Federico II) using both a VG Isomass 54E single collector and a Finnigan MAT 162RP

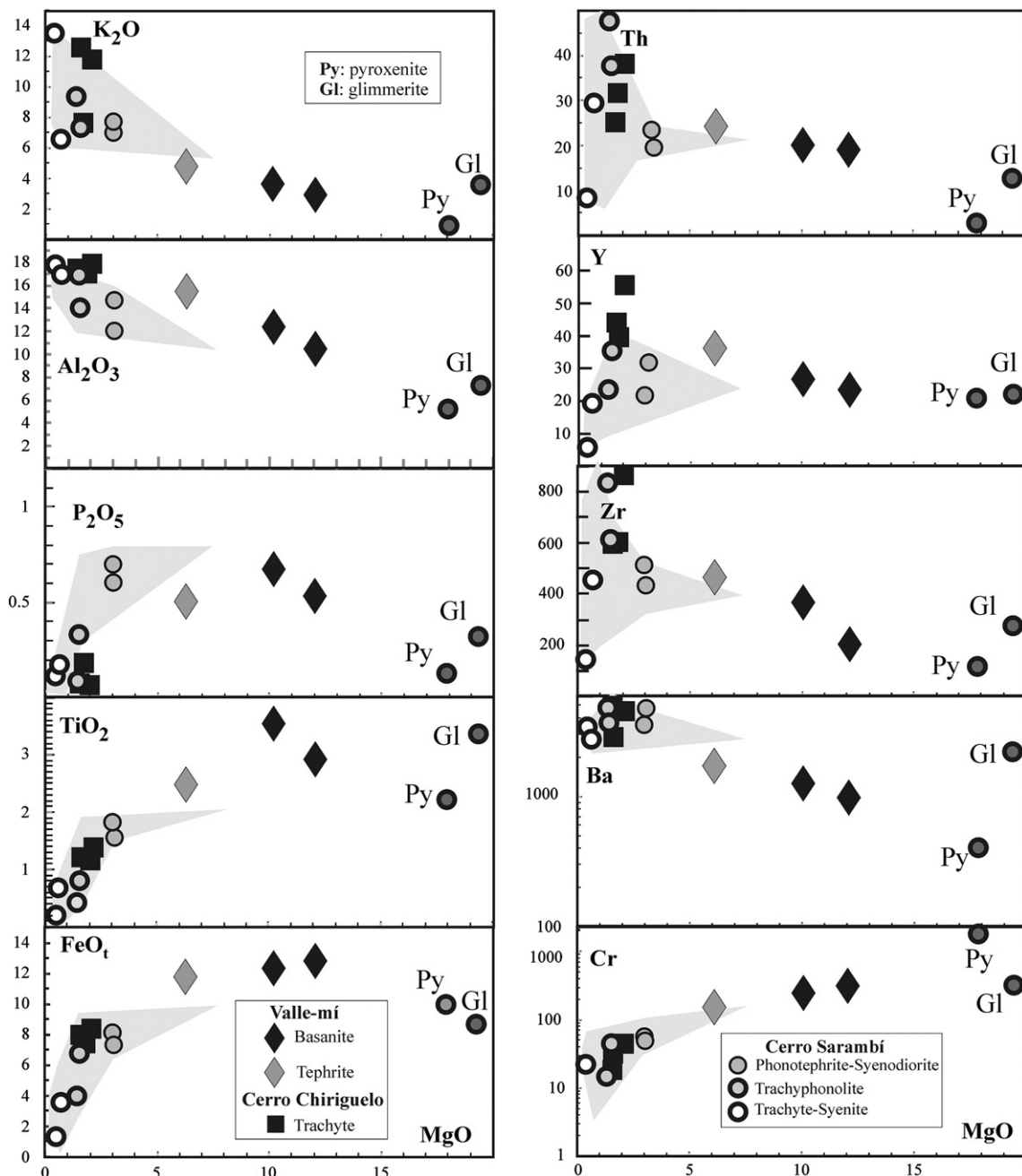


**Fig. 4.** Variation diagram of selected major element oxides (in wt.%) and trace elements (in ppm) for the Rio Apa and Amambay alkaline rocks, using MgO as a differentiation index. Py, pyroxenite; Gl, glimmerite. Grey fields cover the complete range of rock compositions found at Cerro Sarambí (after Gomes et al., 2011).

multicollector mass spectrometers and following the procedures given in Castorina et al. (1996). Repeated analyses of NBS987 Sr and La Jolla Nd isotopic standards yielded average values of  $0.710272 \pm 9$  ( $N = 12$ ) and  $0.511851 \pm 8$  ( $N = 5$ ), respectively. The  $\varepsilon_{\text{d}}\text{Sr}$  and  $\varepsilon_{\text{d}}\text{Nd}$  time-integrated values were calculated using the following values for Bulk Earth:  $^{87}\text{Sr}/^{86}\text{Sr} = 0.7047$ ;  $^{87}\text{Rb}/^{86}\text{Rb} = 0.0827$ ;  $^{143}\text{Nd}/^{144}\text{Nd} = 0.512638$ ;  $^{147}\text{Sm}/^{144}\text{Nd} = 0.1967$  (Faure, 1998).  $T^{\text{DM}}$ , depleted mantle values were calculated according to De Paolo (1988).

Accuracy and precision of the analytical data were reported previously, i.e. by Piccirillo and Melfi (1988), Comin-Chiaromonti and Gomes (1996, 2005), Comin-Chiaromonti et al. (2007a, 2007b, 2007c) and therein references).

## 5. Geochemistry

Major element trends against MgO commonly show inflections at the transition from basanite to tephrite (Fig. 4). Concentrations of  $\text{TiO}_2$  and total Fe are highest in the basanite samples ( $\text{MgO} \approx 10$  wt.%), then decrease strongly in the more evolved samples. Similarly,  $\text{P}_2\text{O}_5$  first increases until about 10 wt.% MgO and then declines sharply with further differentiation. The  $\text{Al}_2\text{O}_3$  and  $\text{K}_2\text{O}$  on the whole increase in the more-evolved samples.  $\text{CaO}$  and  $\text{Sr}$  (not shown in Fig. 4) display scattered trends, probably because of their partitioning into the primary carbonates found in the various rock-types. An apparent scattering of data for the whole Cerro Sarambí population was seen by Gomes et al. (2011) and is probably due to fenitization and hydrothermal processes (Comin-Chiaromonti et al., 2007b).

Trace elements (Fig. 4, Tables 1 to 3) that behave incomparably throughout the compositional range from basanite to phonolite are Rb (41–328 ppm), Th (8–48 ppm), Zr (147–870 ppm), Nb (33–185 ppm) and Ba (793–5334 ppm). Yttrium variations show trends that are similar to those of P and Th suggesting that the decrease in Y in the more evolved samples is due to crystallization of apatite (e.g., Brassines et al., 2005). The behavior of Cr mirrors that of  $\text{FeO}_{\text{tot}}$  and  $\text{TiO}_2$ .

Fig. 5A and B summarize the distribution of incompatible elements and rare earth elements (REE) of the alkaline samples from the three centers in multi-element diagrams normalized to the primitive mantle (Sun and McDonough, 1989) and to the chondrite (Boynton, 1984), respectively. The compositions of other rock-types outcropping in the NPAA are also plotted.

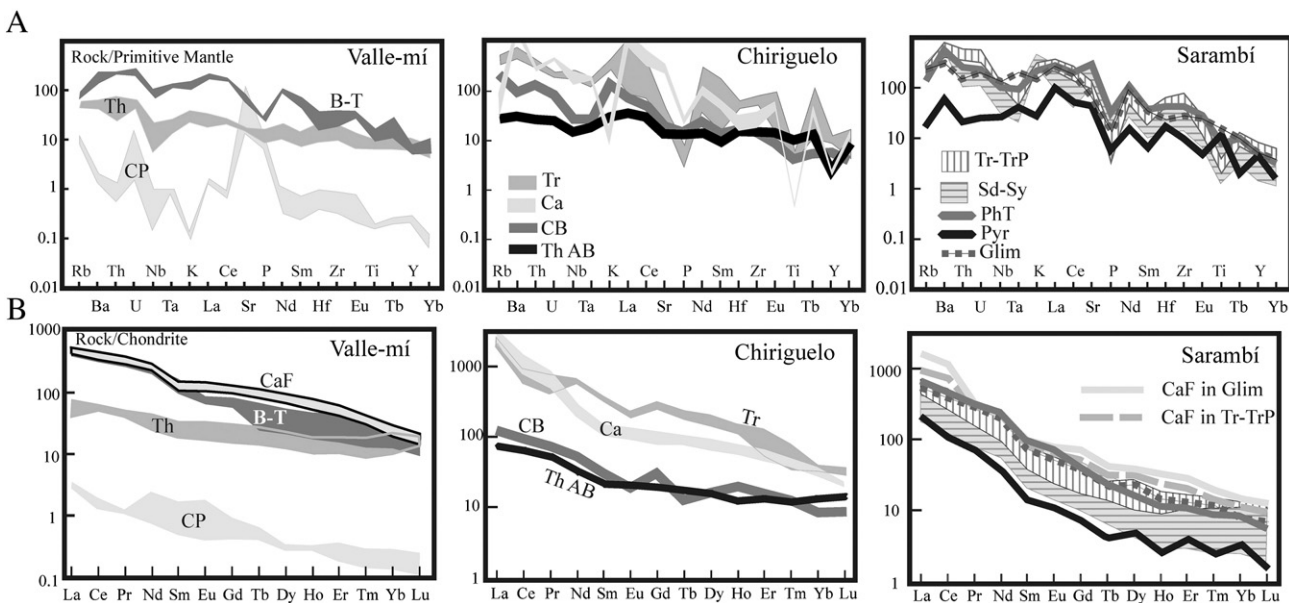


**Fig. 5.** Trace element compositions of the studied rocks. A) Primitive mantle (Sun and McDonough, 1989) normalized, and B) chondrite (Boynton, 1984) normalized rock-types (Table 1 to 3). Valle-mí; B-T, basanite–tephrite; Th, tholeiitic basalts and basaltic andesites; CP, carbonatic platform, Cerro Chiriguelo: Tr, trachytes; Ca, carbonatites; CB, crystalline basement; AB, basaltic andesite; Cerro Sarambí: Tr-TrP, trachytes–trachyphonolites; Sd-Sy, syenodiorites–syenites; PhT, phonotephrite; Pyr, pyroxenite; Glimm, glimmerite; CaF, carbonate fraction.

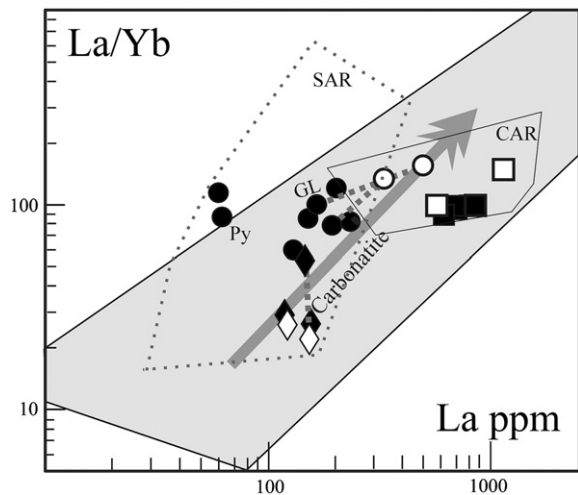


**Fig. 6.** La (ppm) vs. La/Yb ratios for silicate rocks, carbonatites and carbonate fractions from Rio Apa and Amambay regions (discussion in Comin-Chiaromonti et al., 2005a and therein references). Grey area: carbonatite field after Andersen (1987). Full symbols: Valle-mí, diamonds; Cerro Chiriguelo, squares; Cerro Sarambí, circles; open symbols: carbonatites or carbonate fractions; GL, glimmerite; Py, pyroxenite. Tie lines link whole rock compositions with their carbonate fraction. For comparison, the whole field of alkali rocks (SAR) and of carbonatites (CAR) from Eastern Paraguay is shown.

In general, the investigated carbonatites (mainly associated with evolved rocks – trachytes or phonolites) display higher La/Yb ratios and lower La content when compared with those of the associated rocks. Instead, the carbonate fractions from the silicate rock types show slightly higher La and La/Yb (Fig. 6) than those of the corresponding silicate rock (e.g., sample STE-A, Rio Apa; La = 169 vs. 101; La/Yb = 32.4 vs. 28.2).

### 5.1. Valle-mí

The basanite–tephrite dykes (Fig. 5A) are characterized by negative Eu, Nb, P and Ti anomalies. A strong negative Nb–Ta spike for the tholeiitic dykes of the Paraná LIP (Piccirillo and Melfi, 1988) is also shown in the figure. The carbonate platform rocks show very low contents of incompatible elements and REE and particularly of U and Sr. On the

other hand, carbonate fractions from the basanitic dykes show LREE concentrations comparable to those of the host basanitic dykes ( $\text{La/Sm} = 6.33 \pm 0.10$  vs.  $5.80 \pm 0.30$ ; Fig. 5B), but higher MREE and a positive Eu anomaly ( $\text{Eu/Eu}^* = 1.5 \pm 0.4$ ;  $\text{Eu}^* = [\text{Sm}_{\text{CN}} + \text{Gd}_{\text{CN}}]/2$ ; CN = chondrite normalized; Boynton, 1984).

## 5.2. Cerro Chiriguelo

On the whole, the tholeiitic basaltic andesites of the complex show incompatible elements and REE concentrations and patterns similar to those from Valle-mí equivalents (Fig. 5A and B). The crystalline basement is characterized by negative Nb-Ta-Ti and by positive Th-U-K anomalies. The carbonatites contain very high contents of incompatible elements in addition to marked (Rb, K, P and Ti) or moderate (Hf-Zr) negative anomalies. The associated trachytes display strong enrichment of  $\text{K}_2\text{O}$  (up to 12.53 wt.%) and low  $\text{Na}_2\text{O}$  (up to 2.36 wt.%), suggesting a K-rich (basanitic) parental magma that produced a carbonate fraction by crystal fractionation and liquid immiscibility (after Censi et al., 1989; Comin-Chiaromonti et al., 2005b; Kasputin, 1983; Lee and Wyllie, 1998; Woolley, 1982;). In fact, the trachytes show  $\sum \text{REE}$  from 1828 to 2353 ppm vs. 1582 to 2679 ppm in the associated carbonatites and important fractionations of LREE with respect to HREE (ppm  $\text{La/Yb} = 62 \pm 1$  for trachytes and 66–98 for carbonatites). The major difference is that the trachytes have higher MREE and Eu, but with a negative Eu anomaly ( $\text{Eu/Eu}^* = 0.64$ ; probably due to feldspar and sphene fractionation) vs  $\text{Eu/Eu}^* = 1.0$  of the carbonatites (Fig. 5B).

## 5.3. Cerro Sarambí

Incompatible elements normalized to primordial mantle, for both plutonic and volcanic rocks, show positive anomalies for Ba, Th, U, K, Sr, Zr and negative anomalies for Nb-Ta, P and Ti, similar in behavior and concentration to the glimmerite veins (Fig. 5A). On the other hand, the pyroxenite veins contain lower concentrations of Rb to Nb and higher La, Nd, Hf, Eu and Tb.

The REE patterns of the Cerro Sarambí rocks are on the whole depleted with respect to the Cerro Chiriguelo rock types (Cerro Sarambí,  $\Sigma \text{REE}$ , ppm: glimmerite, 688; pyroxenite 193; other silicate rock-types, 213–926; carbonatites  $1491 \pm 368$ ), but with comparable fractionations of LREE/HREE (silicate rocks:  $61 \pm 15$ ; carbonatites:  $98 \pm 10$ ). On the other hand, the  $\text{Eu/Eu}^*$  is around 1 for all rock-types ( $0.93 \pm 0.1$ ).

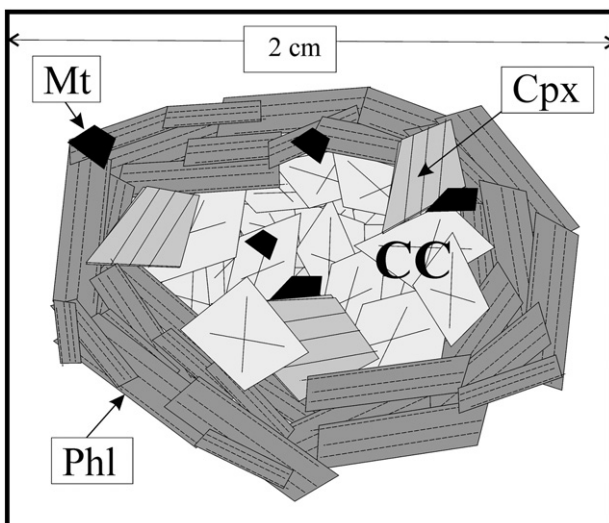


**Fig. 7.** Ocelli-like texture in glimmerites from the Cerro Sarambí complex (sample GL-SA). For comparison see Fig. 10 of Comin-Chiaromonti et al. (2007b). Mt = magnetite; Cpx = clinopyroxene; Phl = phlogopite; CC = carbonate.

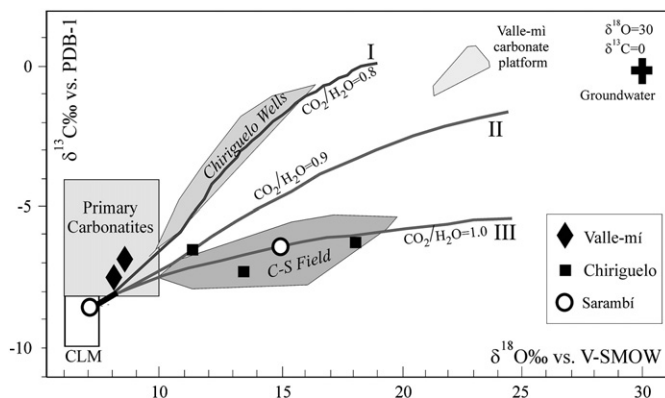


**Fig. 8.** Plot of  $\delta^{18}\text{O}$  against  $\delta^{13}\text{C}$  for the primary carbonates from north-eastern Paraguay, and evolution of the O-C isotope compositions from magmatic (700–400 °C; primary carbonates box) to hydrothermal conditions (400–80 °C; I, II, III lines) at variable  $\text{CO}_2/\text{H}_2\text{O}$  (0.8–1.0, respectively) ratios. Cerro Chiriguelo wells and C-S (Cerro Chiriguelo–Cerro Sarambí) main field as in Censi et al. (1989) and in Comin-Chiaromonti et al. (2005a); data source for Valle-mí carbonate platform and groundwater as in Castorina et al. (1996, 1997). Primary carbonates box after Taylor et al. (1967); CLM, continental lithospheric mantle (Kyser, 1990). Groundwater:  $\delta^{13}\text{C} = 0\text{‰}$ ;  $\delta^{18}\text{O} = 30\text{‰}$  (after Taylor, 1978; Usdowski, 1982; Castorina et al., 1997).

## 5.4. C–O isotopes

Selected data on oxygen and carbon isotopes for carbonatite and carbonate-rich rock types from north-eastern Paraguay are plotted in Fig. 8. Additional sets of data are available in Castorina et al. (1997) and in Comin-Chiaromonti et al. (2005b).

The C–O isotopic composition of the ocelli of the GL-SA sample (Fig. 7; dolomite) from Cerro Sarambí (Table 3, Fig. 8) plots inside the continental lithospheric mantle field (Kyser, 1990), while the sample SA-95B (calcite) plots at high  $\delta^{18}\text{O}$  and relatively low  $\delta^{13}\text{C}$  (along the trend III of Fig. 8) suggesting hydrothermal conditions. Notably, the isotope composition of the carbonate phase from the basanites of Cerro Sarambí plots within the primary carbonatite field of Taylor et al. (1967).

Rocks from Valle-mí and Cerro Chiriguelo display two trends for primary carbonates, both starting from compositions typical of the upper continental mantle (Comin-Chiaromonti et al., 2005a, 2005b): 1) a trend corresponding to carbonates from silicate rocks collected from Cerro Chiriguelo wells (trend I of Fig. 8); 2) a trend that includes carbonatites sampled near, or at, the topographic surface (trend III of Fig. 8; cf. Censi et al., 1989). The two trends intersect at about  $\delta^{18}\text{O} = 8.0$  and  $\delta^{13}\text{C} = -8.0$ , close to the primary carbonatite field of Taylor et al. (1967), indicating a development from magmatic to hydrothermal conditions (cf. Comin-Chiaromonti et al., 2005a,b).

## 5.5. Sr–Nd isotopes

The NPAA alkaline rocks show a relatively restricted distribution in Sr–Nd isotopic space (Fig. 9), overlapping the so called “Paraguay array” defined by Comin-Chiaromonti et al. (2007a) for the composition of the Cretaceous Na- and K-alkaline rocks from central Paraguay that plot parallel to the conventional “mantle array” (e.g., Zindler and Hart, 1986). The alkaline-carbonatite rocks from the NPAA have high initial  $^{87}\text{Sr}/^{86}\text{Sr}_i$  (0.70645 to 0.70794) and low initial  $^{143}\text{Nd}/^{144}\text{Nd}_i$  (0.51151 to 0.51186) and are similar to the carbonatites of the Paraná Basin (Comin-Chiaromonti and Gomes, 1996, 2005).

$^{87}\text{Sr}/^{86}\text{Sr}_i$  and  $^{143}\text{Nd}/^{144}\text{Nd}_i$  of the NPAA tholeiites (Tables 1 to 3) are similar to those of the Eastern Paraguay tholeiites, both low-Ti (L-Ti) and high-Ti (H-Ti) variants (0.70456 to 0.70596 and 0.51225 to 0.51256, respectively; Comin-Chiaromonti et al., 1992, 1997). These values overlap the range of the Early Cretaceous uncontaminated tholeiites from the Paraná Basin continental flood basalts (Fig. 9).

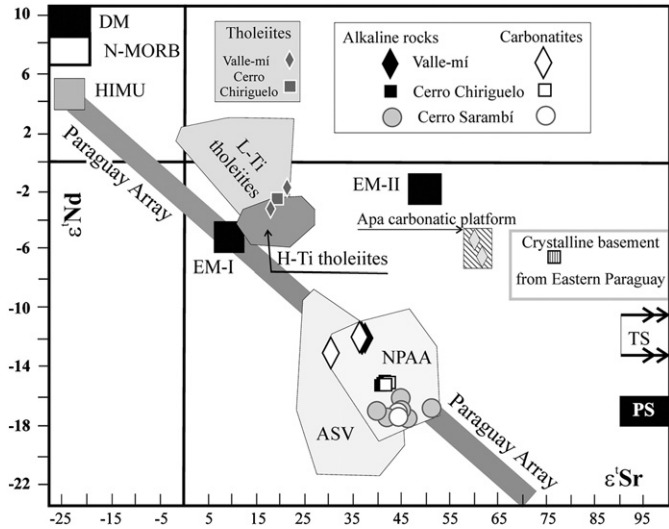


**Fig. 9.** Plot of Sr and Nd isotope in  $\epsilon$ -Sr vs.  $\epsilon$ -Nd notation for igneous rocks from north-eastern Paraguay. Data source: present study, Castorina et al. (1997) and Comin-Chiaromonti et al. (2001, 2007a, and therein references). DM, HIMU, EM-I and EMII mantle components, terrigenous and pelagic sediments, TS and PS, respectively (Zindler and Hart, 1986); crystalline basement (Comin-Chiaromonti et al., 1997). Paraguay array is according to Comin-Chiaromonti et al. (2007a, and therein references); L-Ti and H-Ti tholeiites are from Piccirillo and Melfi (1988), Castorina et al. (1996) and Comin-Chiaromonti et al. (2005a). ASV: alkaline–carbonatic magmatism in the Asunción–Sapucai–Villarrica graben (Comin-Chiaromonti et al., 2007a, b, c); NPAA: alkaline–carbonatitic magmatism from Rio Apa and Amambay Provinces, North-eastern Paraguay (cf. Tables 1–3 and Castorina et al., 1997).

## 6. Discussion

### 6.1. Interaction between silicatic and carbonatitic magmas from NPAA

Considering that the carbonates hosted in the silicate rocks (15–20 wt.%) are late crystallizing phases, and that the carbonatites may represent a liquid exsolved from an evolved magma (such as a phonolite), the total fraction of carbonatitic magma appears to be higher (30–35 wt.%) than the carbonate content in the parental silicate melt. Thus, if Valle-mí basanite is assumed to be the parental magma of the carbonatites, the evolution could have occurred in two steps: 1) crystal fractionation from basanite to trachyphonolite, which explains the concentration of  $\text{CO}_2$  rich fluids and 2) exsolution of carbonatitic liquids (about 20 wt.%, according to Castorina et al., 1997) from the more differentiated magmas. Notably, the C–O isotopes of the calcite–dolomite and apatite–calcite pairs are correlated, and two distinct temperature trends crossing at 920 °C are observed. This temperature appears consistent with those (850–950 °C) estimated by Castorina et al. (1996) for the exsolution of carbonatitic melts from a trachyphonolitic magma at pressures  $\leq 1.0$  Kbar. On the basis of these considerations, Castorina et al. (1997) suggested an increasing fraction of carbonate dissolved in silicate liquids, up to the exsolution of an immiscible carbonatitic melt, following the trend basanite → phonotephrite → trachyphonolite–phonolite (trachyte) → carbonatite. This evolution also explains the development from magmatic to hydrothermal conditions which occur because after the crystallization of the primary carbonate, the  $\text{CO}_2$  bearing fluids often interact again with the primary carbonate and fenitize the country rocks following paths depending on temperature and the water/rock ratio.

The O–C isotopic variations, related to hydrothermal water/rock interaction are shown in Fig. 8 (trends I, II, III). Trends are positively correlated, but trend I, representing sub-intrusive conditions, is more steeper than trends II and III, representing surface specimens (nearly flat). Considering surface conditions with  $\text{CO}_2/\text{H}_2\text{O} \sim 2.0$  both trend are consistent with hydrothermal temperature from 400 to 80 °C and suggest a variable involvement of non-mantle derived material

(Castorina et al., 1997) being the lowest  $\delta^{13}\text{C}$  values related to hydrolysis of biogenetic C and modifying the  $\text{CO}_2/\text{H}_2\text{O}$  ratio from 0.8 (trend I) to 1.0 (trend II).

If the differentiation of the  $\text{CO}_2$ -bearing melts is relatively restricted (i.e., basanite to phonotephrite), the proportion of exsolved carbonatitic melt is relatively small and crystallizes *in situ*, forming patches or ocelli in the host alkaline rock (as shown in Fig. 7).

Finally, it is worth noting that  $\text{CaO}/\text{Al}_2\text{O}_3$  vs.  $\text{La/Yb}$  and  $\text{Ti/Eu}$  diagrams indicate that the primitive rocks from the carbonatite-free and carbonatite-bearing complexes, respectively, plot in distinct fields (cf. Fig. 7 of Comin-Chiaromonti et al., 2007b; Castorina et al., 1997; Morbidelli et al., 2000).

### 6.2. Mantle source of NPAA silicate and carbonatite magmas

Due to the high Sr and relatively high Nd concentrations of the less-evolved alkaline rocks and associated carbonatites (1000–13000 and 160–300 ppm, respectively), Comin-Chiaromonti et al. (1999) suggested that initial Sr–Nd isotopic ratios of the investigated rocks are little affected by crustal contamination and, as a result, can be considered as primary compositions derived from an enriched mantle source. According to Piccirillo et al. (1989) and Comin-Chiaromonti et al. (1997), these alkaline rocks probably acquired lithospheric mantle components which have been variously enriched during the past orogenesis that interested the south American platform (i.e., Eburnean cycle, ca. 2.2–2.0 Ga; Statherian taphrogenesis, ca. 1.8–1.75 Ga; Grenvillian orogenesis, ca. 1.3–1.1 Ga; and Brazilian–Pan-African cycle, ca 0.9–0.5 Ga). In particular, the K-alkaline–carbonatite rocks from the NPAA and the Asunción–Sapucai–Villarrica graben (central Paraguay) which, respectively, pre- (138 Ma) and post-date (121–128 Ma) the main tholeiitic event (133 Ma) preferentially sampled the (most) enriched mantle domains.

The  $T^{\text{DM}}$  (Nd) model ages calculated for the studied rocks, as well as for the Paraná Basin tholeiites and associated Brazilian alkaline–carbonatitic rocks, further constrain the age of the mantle enrichment processes (Comin-Chiaromonti and Gomes, 2005; Comin-Chiaromonti et al., 1997; Gastal et al., 2005; Rosset et al., 2007). In particular, it should be noted that: 1) the high-Ti flood tholeiites and dyke swarms from the Paraná Basin, as well as the Brazilian Na carbonatite bearing complexes such as Jaquiá, yield  $T^{\text{DM}}$  (Nd) model ages ranging mainly from 0.5 to 2.1 Ga with a mean-peak at  $1.1 \pm 0.1$  and  $0.98 \pm 0.1$  Ga, respectively. 2) The Early Cretaceous potassic rocks and carbonatites from central-eastern Paraguay show a similar interval of  $T^{\text{DM}}$  (Nd) model ages (0.9 to 2.1 Ga) with a mean-peak at  $1.5 \pm 0.2$  Ga. 3) The Early Cretaceous K-alkaline rocks and carbonatites from NPAA range from 1.5 to 2.3 Ga (mean  $1.6 \pm 0.3$  Ga). 4) The low-Ti tholeiites show a major variation in  $T^{\text{DM}}$ , ranging from 0.7 to 2.4 Ga with a mean peak of  $1.6 \pm 0.3$  Ga. Therefore, in general, the model ages indicate that some different “metasomatic events” may have occurred from the Paleoproterozoic to the Neoproterozoic as precursors of alkaline and tholeiitic magmas in the Paraná Basin (Comin-Chiaromonti and Gomes, 2005; Cordani et al., 2010). This conclusion is further supported by other observations: the overlap of isotopic compositions for different igneous rocks (i.e., alkaline rocks and carbonatites) cannot be accidental and points to sampling of ancient reservoirs formed at different times within the same sub-continental lithospheric mantle (Carlson et al., 1996; Foley, 1992a, b) or to recycling of crustal materials subducted during various subduction events (Menzies, 1990; Weaver, 1991). This could also explain why all the investigated rocks, excluding pyroxenite veins, are characterized by negative Nb–Ta anomalies which would suggest a subduction setting (cf. Beccaluva et al., 1991; Pearce, 1983) while strong geological and geophysical evidence indicate that the NPAA rocks are related to an extensional tectonics. Similar characteristics (e.g., N–Ta depletion) are also shown by the Early Cretaceous alkaline–carbonatite complexes of central-eastern Paraguay and by the alkaline and tholeiitic magmatic

rock occurrences from the eastern portion of the Paraná Basin (cf. also Comin-Chiaromonti et al., 1999).

According to Antonini et al. (2005), a veined lithospheric mantle (amphibole/phlogopite–carbonate–lherzolite and amphibole–lherzolite + CO<sub>2</sub>-fluid, type III and IV veins of Meen et al., 1989) of Proterozoic age may well account for the alkaline and tholeiitic magmatism of the entire Paraná–Etendeka LIP and of the NPAA alkaline and carbonatitic magmas, in particular. The alkaline–carbonatitic magmas may be issued from mantle domains metasomatized by small-volume melts and fluids rich in incompatible elements that formed a vein network variously enriched in LILE and LREE (see Foley, 1992a,b). The peridotite matrix (depleted component) and the newly formed veins (enriched component) possibly followed different isotopic evolutionary paths, which is particularly reflected by the high <sup>87</sup>Sr/<sup>86</sup>Sr of the primary carbonates. The involvement of mantle sources, likely within the subcontinental lithospheric mantle, which preserved isotopic heterogeneities formed over long time periods could explain the variable enrichment observed in the Paraná–Etendeka LIP and particularly in its alkaline–carbonatitic magmatism.

## 7. Concluding remarks

- 1) The K-alkaline–carbonatite rocks which pre-date the Paraná tholeiitic event (138–139 Ma), are structurally controlled by the Rio Apa antiform and by the Jejui–Aguaray–Guazu fault system. They intruded the Rio Apa and Amambay regions in north-eastern Paraguay. The rock-types of potassic affinity range from basanite to trachyte and trachyphonolite (and intrusive equivalents), the latter being sometimes locally fenitized. Glimmerite and pyroxenite veins are found in the Cerro Sarambí complex (Castorina et al., 1997).
- 2) Excluding pyroxenite veins, the alkaline and tholeiitic rocks from NPAA are characterized by negative Nb–Ta anomalies. Significant variations in O–C isotope composition of primary carbonates from potassic rock-types are observed, i.e. values ranging from close to the field of the continental lithospheric mantle (carbonate fraction from a glimmerite vein), or close to the field of primary carbonatites (basanites), to values typical of hydrothermal environments; the latter is observed particularly in quite differentiated magma types (trachytes I.s. from Cerro Chiriguelo and Cerro Sarambí).
- 3) Geochemical data (e.g., La vs La/Yb and O–C isotopes) show a magmatic evolution following two main trends: 1) basanite → trachyphonolite, leading to differentiated rock-types by fractional crystallization and to an increase in the concentration of CO<sub>2</sub> in the fluids; 2) exsolution of about 30–35 wt.% of carbonatitic liquids from phonolitic–trachytic magmas, as clearly apparent in the Chiriguelo Complex.
- 4) Sr–Nd isotopes show that K-alkaline magmas and associated carbonatites reflect the composition of the mantle source with a progressive enrichment from Valle-mí basanites to Cerro Sarambí rock-types. In particular, Sr–Nd isotopes indicate that the carbonatite system was derived from enriched mantle sources, without significant crustal contamination.
- 5) The genesis of the investigated alkaline magmas probably required a mantle veined by ancient metasomatic events coincident with the main orogenic events in the South American plate as suggested by the T<sup>DM</sup> (Nd) model ages.

## Acknowledgements

P.C.C. gratefully acknowledges CNR and MIUR (Italian Agencies) for financial support since 1981, and the Department of Mathematics and Geosciences of the Trieste University for the use of chemical laboratories. Thanks are due to engineer E. Debenardi (deceased) and to geologists D. Orué, Luis Lúcia and L.A. Martinez for their collaborations. We thank J. Kynicky for useful comments on early versions of this manuscript and acknowledge the constructive reviews of D.R. Baker, J. Mata,

A. Marzoli and an anonymous reviewer. Editorial assistance of A. Marzoli and A. Kerr helped improving the early versions of the manuscript. This research was supported by grants (Procs. 08/3807-4 and 10/50887-3) to C.B. Gomes from the Brazilian Agency Fapesp. This paper is dedicated to the memory of Enzo Michele Piccirillo who substantially contributed to the understanding of the Paraná magmatism.

## References

- Andersen, T., 1987. Mantle and crustal components in a carbonatite complex, and the evolution of carbonatite magma: REE and isotopic evidence from the Fen complex, southeast Norway. *Chemical Geology: Isotope Geoscience* 65, 147–166.
- Antonini, P., Gasparon, M., Comin-Chiaromonti, P., Gomes, C.B., 2005. Post-Paleozoic magmatism in Eastern Paraguay: Sr–Nd–Pb isotope compositions. In: Comin-Chiaromonti, P., Gomes, C.B. (Eds.), Mesozoic to Cenozoic Alkaline Magmatism in the Brazilian Platform. Edusp/Fapesp, São Paulo, pp. 57–70.
- Beccaluva, L., Di Girolamo, P., Serri, G., 1991. Petrogenesis and tectonic setting of the Roman Volcanic Province, Italy. *Lithos* 26, 191–221.
- Bellieni, G., Comin-Chiaromonti, P., Marques, L.S., Martinez, L.A., Melfi, A.J., Nardy, A.J.R., Piccirillo, E.M., 1986. Continental flood basalts from the central-eastern regions of the Paraná plateau (Paraguay and Argentina): petrogenetic aspects. *Neues Jahrbuch für Mineralogie (Abhandlungen)* 154, 111–139.
- Boynton, W.V., 1984. Cosmochemistry of the Rare Earth elements: meteorite studies. In: Henderson, P. (Ed.), *Rare Earth Element Geochemistry*. Elsevier, Amsterdam, pp. 63–114.
- Brassines, S., Balaganskaya, E., Demaiffe, D., 2005. Magmatic evolution of the differential ultramafic, alkaline and carbonatite intrusion of Vuoriyarvi (Kola Peninsula, Russia). *A LA-ICP-MS study of apatite*. *Lithos* 85, 76–92.
- Campanha, G.A.C., Warren, L., Boggiani, P.C., Grohmann, C.H., Cáceres, A.A., 2010. Structural analysis of the Itapucumí Group in the Vallemí region, Northern Paraguay: evidence of a New Brasiliano–Pan-African Mobile Belt. *Journal of South American Earth Sciences* 30, 1–11.
- Carlson, R.W., Esperança, S., Svisero, D.P., 1996. Chemical and Os isotopic study of Cretaceous potassic rocks from southern Brazil. *Contributions to Mineralogy and Petrology* 125, 393–405.
- Castorina, F., Censi, P., Barbieri, M., Comin-Chiaromonti, P., Cundari, A., Gomes, C.B., Pardini, G., 1996. Carbonatites from Eastern Paraguay: a comparison with the coeval carbonatites from Brazil and Angola. In: Comin-Chiaromonti, P., Gomes, C.B. (Eds.), *Alkaline Magmatism in Central-Eastern Paraguay. Relationships with Coeval Magmatism in Brazil*. Edusp/Fapesp, São Paulo, pp. 231–248.
- Castorina, F., Censi, P., Comin-Chiaromonti, P., Gomes, C.B., Piccirillo, E.M., Alcover Neto, A., Almeida, R.T., Spezziale, S., Toledo, M.C., 1997. *Geochemistry of carbonatites from Eastern Paraguay and genetic relationships with potassic magmatism: C, O, Sr and Nd isotopes*. *Mineralogy and Petrology* 61, 237–260.
- Censi, P., Comin-Chiaromonti, P., De Marchi, G., Longinelli, A., Orué, D., 1989. *Geochemistry and C–O isotopes of the Chiriguelo carbonatite, northeastern Paraguay*. *Journal of South American Earth Sciences* 2, 295–303.
- Comin-Chiaromonti, P., Gomes, C.B. (Eds.), 1996. *Alkaline Magmatism in Central-Eastern Paraguay. Relationships with Coeval Magmatism in Brazil*. Edusp/Fapesp, São Paulo (464 pp.).
- Comin-Chiaromonti, P., Gomes, C.B. (Eds.), 2005. *Mesozoic to Cenozoic Alkaline Magmatism in the Brazilian Platform*. Edusp/Fapesp, São Paulo (752 pp.).
- Comin-Chiaromonti, P., Cundari, A., Gomes, C.B., Piccirillo, E.M., Censi, P., De Min, A., Bellieni, G., Velázquez, V.F., Orué, D., 1992. Potassic dyke swarm in the Sapucaí graben, Eastern Paraguay: petrographical, mineralogical and geochemical outlines. *Lithos* 28, 283–301.
- Comin-Chiaromonti, P., Cundari, A., De Min, A., Gomes, C.B., Velázquez, V.F., 1996. *Magmatism in Eastern Paraguay: occurrence and petrography*. In: Comin-Chiaromonti, P., Gomes, C.B. (Eds.), *Alkaline magmatism in central-eastern Paraguay. Relationships with coeval magmatism in Brazil*. Edusp/Fapesp, São Paulo, pp. 103–122.
- Comin-Chiaromonti, P., Cundari, A., Piccirillo, E.M., Gomes, C.B., Castorina, F., Censi, P., De Min, A., Marzoli, A., Petrini, R., Spezziale, S., 1997. Potassic and sodic igneous rocks from Eastern Paraguay: their origin from the lithospheric mantle and genetic relationships with the associated Paraná flood tholeites. *Journal of Petrology* 34, 495–528.
- Comin-Chiaromonti, P., Cundari, A., De Graff, J.M., Gomes, C.B., Piccirillo, E.M., 1999. Early Cretaceous–Tertiary magmatism in Eastern Paraguay (western Paraná basin): geological, geophysical and geochemical relationships. *Journal of Geodynamics* 28, 375–391.
- Comin-Chiaromonti, P., De Min, A., Girardi, V.A.V., Ruberti, E., 2001. Post-paleozoic magmatism in Angola and Namibia: a review. In: Beccaluva, L., Bianchini, G., Wilson, M. (Eds.), *Volcanism and Evolution of the African Lithosphere*. The Geological Society of America Special Paper, 478, pp. 233–247.
- Comin-Chiaromonti, P., Gomes, C.B., Censi, P., Spezziale, S., 2005a. Carbonatites from southeastern Brazil: a model for the carbon and oxygen variations. In: Comin-Chiaromonti, P., Gomes, C.B. (Eds.), *Mesozoic to Cenozoic alkaline magmatism in the Brazilian Platform*. Edusp/Fapesp, São Paulo, pp. 629–656.
- Comin-Chiaromonti, P., Gomes, C.B., Marques, L.S., Censi, P., Ruberti, E., Antonini, P., 2005b. Carbonatites from southeastern Brazil: Geochemistry, O–C, Sr–Nd–Pb isotopes and relationships with the magmatism from the Paraná–Angola–Namibia Province. In: Comin-Chiaromonti, P., Gomes, C.B. (Eds.), *Mesozoic to Cenozoic Alkaline Magmatism in the Brazilian Platform*. Edusp/Fapesp, São Paulo, Brazil, pp. 657–688.
- Comin-Chiaromonti, P., Marzoli, A., Gomes, C.B., Milan, A., Riccomini, C., Mantovani, M.M.S., Renne, P., Tassinari, C.C.G., Vasconcelos, P.M., 2007a. *Origin of post Paleozoic*

- magma in Eastern Paraguay. In: Foulger, G.R., Jurdy, D.M. (Eds.), Plates, plumes, and planetary processes. The Geological Society of America Special Paper, 430, pp. 603–633.
- Comin-Chiaromonti, P., Gomes, C.B., Cundari, A., Castorina, F., Censi, P., 2007b. A review of carbonatitic magmatism in the Paraná–Angola–Namibia (PAN) system. *Periodico di Mineralogia* 76, 25–78.
- Comin-Chiaromonti, P., Gomes, C.B., De Min, A., Ernesto, M., Marzoli, A., Riccomini, C., 2007c. Eastern Paraguay: an overview of the post-Paleozoic magmatism and geodynamic implications. *Rend. Fis. Acc. Lincei*, 9, 18 139–192.
- Comin-Chiaromonti, P., De Min, A., Girardi, V.A.V., Ruberti, E., 2011. Post-Paleozoic magmatism in Angola and Namibia: a review. In: Beccaluva, L., Bianchini, G., Wilson, M. (Eds.), Volcanism and evolution of the African lithosphere. Geological Society of America Special Paper, 478, pp. 223–247.
- Cordani, U.G., Tassinari, C.C.G., Rolim, D.R., 2005. The basement of the Rio Apa Craton in Mato Grosso do Sul (Brazil) and northern Paraguay: a geochronological correlation with the tectonic provinces of the south-western Amazonian Craton. *Gondwana Conference, Abstracts volume, Mendoza, Argentina*, pp. 1–12.
- Cordani, U.G., Teixeira, W., Tassinari, C.C.G., Coutinho, J.M.V., Ruiz, A.S., 2010. The Rio Apa Craton in Mato Grosso (Brazil) and Northern Paraguay: Geochronological evolution, correlations and tectonic implications from Rodinia and Gondwana. *American Journal of Science* 310, 981–1023.
- De La Roche, H., Leterrier, J., Grandclaude, P. e, Marchal, M., 1980. A classification of volcanic and plutonic rocks using R1–R2 diagram and major-element analyses: its relationships with current nomenclature. *Chemical Geology* 29, 183–210.
- De Paolo, D.J., 1988. Age dependence of the composition of continental crust as determined from Nd isotopic variations in igneous rocks. *Earth and Planetary Science Letters* 59, 263–271.
- Faure, G., 1998. Principles and applications of geochemistry. Prentice Hall, Bergen County, New Jersey, USA (600 pp.).
- Foley, S., 1992a. Potassic and ultrapotassic magmatism and their origin. *Lithos* 28, 181–186.
- Foley, S., 1992b. Veins-plus-wall rock melting mechanism in the lithosphere and the origin of potassic alkaline magmas. *Lithos* 28, 435–453.
- Gastal, M.P., Lafon, J.M., Hartmann, L.A., Koester, E., 2005. Sm–Nd isotopic investigation of Neoproterozoic and Cretaceous igneous rocks from southern Brazil: a study of magmatic processes. *Lithos* 82, 345–377.
- Gibson, S.A., Thompson, R.N., Day, J.A., 2006. Timescales and mechanisms of plume lithosphere interactions:  $^{40}\text{Ar}/^{39}\text{Ar}$  geochronology and geochemistry of alkaline igneous rocks from the Paraná–Etendeka large igneous province. *Earth and Planetary Science Letters* 251, 1–17.
- Gomes, C.B., Velázquez, V.F., Azzone, R.G., Paula, G.S., 2011. Alkaline magmatism in the Amambay area, NE Paraguay. The Cerro Sarambí complex. *Journal of South American Earth Sciences* 32, 75–95.
- Haggerty, S.E., Mariano, A.N., 1983. strontian loparite and strontio-chevkinite: two new minerals in rheomorphic fenites from the Paraná Basin carbonatites, South America. *Contributions to Mineralogy and Petrology* 84, 365–381.
- Kasputin, Y.L., 1983. Strontium and barium geochemistry in carbonatite complexes. *Geokhimiya* 57, 41–62.
- Kysar, T.K., 1990. Stable isotopes in the continental lithospheric mantle. In: Menzies, M.A. (Ed.), Continental Mantle. Clarendon Press, Oxford, pp. 127–156.
- Le Bas, M.J., 1981. Carbonatite magmas. *Mineralogical Magazine* 44, 133–140.
- Le Maitre, R.P., 1989. A Classification of Igneous Rocks and Glossary of Terms. Blackwell, Oxford (193 pp.).
- Lee, W.-J., Wyllie, P., 1998. Petrogenesis of carbonatite magmas from Mantle to Crust, constrained by the system  $\text{CaO} - (\text{MgO} + \text{FeO}^*) - (\text{Na}_2\text{O} + \text{K}_2\text{O}) - 8\text{SiO}_2 + \text{Al}_2\text{O}_3 + \text{TiO}_2 - \text{CO}_2$ . *Journal of Petrology* 39, 496–517.
- Livieres, R.A., Quade, H., 1987. Distribución regional y asentamiento tectónico de los complejos alcalinos del Paraguay. *Zentralblatt für Geologie und Paläontologie* 7 (8), 791–805.
- Meen, J.K., Ayers, J.C., Fregeau, E.J., 1989. A model of mantle metasomatism by carbonated alkaline melts: trace element and isotopic compositions of mantle source regions of carbonatite and other continental igneous rocks. In: Bell, K. (Ed.), Carbonatites, genesis and evolution. Unwin Hyman, London, pp. 464–499.
- Menzies, M.A. (Ed.), 1990. Continental Mantle. Oxford Clarendon Press, Oxford (450 pp.).
- Morbidelli, L., Gomes, C.B., Beccaluva, L., Brotzu, P., Conte, A., Ruberti, E., Traversa, G., 2000. The Paríquera Açu K-alkaline complex and southern Brazil lithospheric mantle source characteristics. *Journal of Asian Earth Sciences* 18, 129–150.
- Palmieri, J.H., Velázquez, J.C., 1982. Geología del Paraguay. Serie Ciencias Naturales, NAPA, Asunción. (65 pp.).
- Pearce, J.A., 1983. Role of sub-continental lithosphere in magma genesis at active continental margins. In: Hawkesworth, C.J., Norry, M.J. (Eds.), Continental Basalts and Mantle Xenoliths. Shiva, Nantwich, UK, pp. 230–249.
- Piccirillo, E.M., Melfi, A.J. (Eds.), 1988. The Mesozoic Flood Volcanism of the Paraná Basin: Petrogenetic and Geophysical Aspects. IAG, São Paulo (600 pp.).
- Piccirillo, E.M., Civetta, L., Petrini, R., Longinelli, A., Bellieni, G., Comin-Chiaromonti, P., Marques, L.S., Melfi, A.J., 1989. Regional variations within the Paraná flood basalts (southern Brazil): evidence for subcontinental mantle, heterogeneity and crustal contamination. *Chemical Geology* 75, 103–122.
- Rosset, A., De Min, A., Marques, L.S., Macambira, M.J.B., Ernesto, M., Renne, P.R., Piccirillo, E.M., 2007. Genesis and geodynamic significance of Mesoproterozoic and Early Cretaceous tholeiitic dyke swarms from the São Francisco Craton (Brazil). *Journal of South American Earth Sciences* 24, 69–92.
- Rowell, M.J., 1995. Colorimetric method for  $\text{CO}_2$  measurement in soils. *Soil Biology and Biochemistry* 27, 373–375.
- Sun, S.S., McDonough, W.F., 1989. Chemical and isotopic systematics of oceanic basalts. In: Saunders, D., Norry, M.J. (Eds.), Magmatism in the ocean basins. Geological Society of America Special Paper, 42, pp. 313–345.
- Taylor Jr., H.O., 1978. Water/rock interactions and origin of  $\text{H}_2\text{O}$  in granitic batholiths. *Journal of the Geological Society of London* 133, 509–558.
- Taylor Jr., H.P., Frechen, J., Degens, E.T., 1967. Oxygen and carbon isotope studies of carbonatites from the Laacher See District, West Germany and the Alnö District, Sweden. *Geochimica et Cosmochimica Acta* 31, 407–430.
- Usdowski, E., 1982. Reaction and equilibria in the system  $\text{CO}_2 - \text{H}_2\text{O}$  and  $\text{CaCO}_3 - \text{CO}_2 - \text{H}_2\text{O}$  ( $0^\circ$ – $50^\circ$ ). A review. *Neues Jahrbuch für Mineralogie, Abhandlungen* 144, 148–171.
- Weaver, B.L., 1991. The origin of ocean island basalt end-member compositions: trace element and isotopic constraints. *Earth and Planetary Science Letters* 104, 381–397.
- Woolley, A.R., 1982. A discussion of carbonatite evolution and nomenclature, and the generation of sodic and potassic fenites. *Mineralogical Magazine* 46, 13–17.
- Zindler, A., Hart, S., 1986. Chemical geodynamics. *Annual Review of Earth and Planetary Sciences* 14, 493–571.